V European Conference on Computational Fluid Dynamics
ECCOMAS CFD 2010
J. C. F. Pereira and A. Sequeira (Eds)
Lisbon, Portugal, 14–17 June 2010

A PRESSURE-BASED ALGORITHM FOR THE NUMERICAL SOLUTION OF THE INCOMPRESSIBLE NAVIER-STOKES EQUATIONS

Salman Okhovat[*], Ali Ashrafizadeh[†]

[*, †]DOS Lab, K. N. Toosi University of Tech., Faculty of Mechanical Engineering,
No. 17, Pardis Street, Vanak Square, Postal Code: 19991 43344, Tehran, Iran.

[*]e-mail: okhovat@dena.kntu.ac.ir

[†]e-mail: ashrafizadeh@kntu.ac.ir

Key words: Computational Fluid Dynamics, Incompressible flow, Pressure-Based Algorithm, Control-Volume Finite Element Method

Abstract. *A control-volume finite element formulation is proposed for the numerical solution of incompressible laminar flow of Newtonian fluids on 2-D unstructured grids. A collocated arrangement of dependent variables is used and oscillatory solutions are prevented by using the momentum interpolation scheme for mass carrying velocity components in the continuity equation. Bi-linear shape functions in triangular element combined with a physical-based discretization scheme are used to simulate the integration point diffusion and advection fluxes. Benchmark numerical solutions and experimental data are used to validate the proposed numerical solution method. Computational results are in good agreement with the reference data.*

1 INTRODUCTION

The fundamental equations which govern the flow of fluids are the equations for mass, momentum and energy conservation. In two dimensional cases, there are four unknowns, i.e. pressure P, velocity components u and v, and temperature T, which should be obtained simultaneously from the solution of the governing equations. In the pressure-based solution strategy the density (ρ) as well as other thermo-physical variables such as viscosity (μ) are obtained from the relevant state equations.

In incompressible flow, the density is constant and the temperature field does not have any effect on the continuity and momentum equations. Thus, the temperature field is no longer an unknown and the energy equation is redundant. The set of equations for an incompressible flow in a two-dimensional solution domain includes the continuity, x-momentum and y-momentum. The three dependent variables, i.e. u, v and P, are coupled in an incompressible flow field. However, while the momentum balance equations constrain the velocity components, there is apparently no explicit constraint on the pressure field. The pressure is indirectly constrained by the continuity equation. The pressure, therefore, needs to play a role in the momentum equations such that a divergence-free velocity field is obtained.

The numerical modeling of the coupling between the pressure and velocity fields in incompressible flow is not a trivial task and carelessly designed discretization schemes are prove to physically meaningless oscillatory solutions.

Several numerical solution strategies have been proposed to tackle the pressure-velocity coupling problem in incompressible flows. An effective remedy to the decoupling symptom, i.e. the use of a staggered grid arrangement, was proposed by Patankar and Spalding[2] among others. On a staggered grid, the pressure and velocity are not calculated at the same nodal position. In spite of its effectiveness, the staggered grid strategy has a number of shortcomings including the implementation difficulties on unstructured meshes. The first successful co-located method, initially implemented on a structured grid, was proposed by Rhie and Chow[3]. Chorin[4] has also proposed a solution methodology based on the velocity projection concept. There are also other methods which solve the original governing equations simultaneously in a coupled manner[5,6]. In the coupled solution strategy special solution methods, suitable for the solution of ill-conditioned linear equations, are employed and other numerical techniques and tools such as re-ordering, preconditioning and convergence accelerators are often necessary[7]. In nearly all of these developments, structured grids were employed originally.

Incompressible flow solution algorithms on unstructured grids have also been developed during the past decades[8,9,10,11,12], mostly in response to the need for solving flow problems in geometrically complex domains.

Acharya et al.[13] have provided a comprehensive review of pressure-based finite-volume methods in computational fluid dynamics. Furthermore, Kwak et al.[14] describe some of the computational challenges regarding the numerical solution of viscous incompressible flows.

In this paper we propose a control-volume finite element method (CVFEM) formulation for the numerical solution of incompressible laminar flows of Newtonian fluids on 2D unstructured collocated grids. The CVFEM was proposed by Baliga[15] and employed by many others including Schneider and Raw[16] and Karimian et al.[17]. In a CVFEM solution procedure, discretizatin is basically carried out in two major steps. In the first step the governing equations are integrated over the control volumes and in the second step the integration point flux terms are related to the nodal point variables. The proposed algorithm is implemented on a triangular unstructured grid and borrows features from the projection method[4] and the momentum interpolation technique[3,10] to tightly couple the pressure and velocity fields. The power law scheme, modified for triangular meshes, is used to properly model the advection and diffusion transport in the flow field. Boundary condition implementation is described in details and satisfactory numerical results on a number of standard test cases are reported.

2 THE FIRST LEVEL OF DISCRETIZATION: FINITE VOLUME METOD

The conservation equations governing laminar, incompressible Newtonian fluid flow can be expressed in vector form as

$$\frac{\partial \vec{q}}{\partial t}+\frac{\partial \vec{f}_c}{\partial x}+\frac{\partial \vec{g}_c}{\partial y}=\frac{\partial \vec{f}_v}{\partial x}+\frac{\partial \vec{g}_v}{\partial y}+\vec{S} \tag{1}$$

Where the conserved quantity vector $\vec{q}$, the convection flux vectors $\vec{f}_c, \vec{g}_c$, the diffusion flux vectors $\vec{f}_v, \vec{g}_v$, and the source term vector $\vec{S}$ are defined as follows:

$$\vec{q}=\begin{Bmatrix}\rho\\ \rho u\\ \rho v\end{Bmatrix},\ \vec{f}_c=\begin{Bmatrix}\rho u\\ (\rho u)u\\ (\rho u)v\end{Bmatrix},\ \vec{g}_c=\begin{Bmatrix}\rho v\\ (\rho v)u\\ (\rho v)v\end{Bmatrix},\ \vec{f}_v=\begin{Bmatrix}0\\ \tau_{xx}\\ \tau_{xy}\end{Bmatrix},\vec{g}_v=\begin{Bmatrix}0\\ \tau_{yx}\\ \tau_{yy}\end{Bmatrix},\vec{S}=\begin{Bmatrix}S_m\\ \partial P/\partial x+S_u\\ \partial P/\partial y+S_v\end{Bmatrix} \tag{2}$$

The components of the stress tensor are related to the velocity derivatives using the Newtonian fluid assumption as follows:

$$\begin{aligned}&\tau_{xx}=2\mu\frac{\partial u}{\partial x}-\frac{2}{3}\mu\left(\frac{\partial u}{\partial x}+\frac{\partial v}{\partial y}\right),\ \tau_{yy}=2\mu\frac{\partial v}{\partial y}-\frac{2}{3}\mu\left(\frac{\partial u}{\partial x}+\frac{\partial v}{\partial y}\right),\\ &\tau_{xy}=\tau_{xy}=\mu\left(\frac{\partial u}{\partial y}+\frac{\partial v}{\partial x}\right)\end{aligned} \tag{3}$$

The solution domain is discretized by a number of triangle elements. A control volume, defined around a nodal point, is shown in Fig. 1. Each control volume has a number of faces represented by mid points, also called the integration points. The incompressible governing equations are discretized by integrating Eq. (1) over the control volume displayed by the shaded area in Fig. 1.

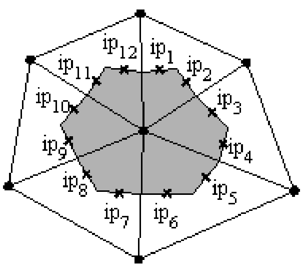

Figure 1: Control volume around a nodal point.

$$\oint_{\forall} \frac{\partial \vec{q}}{\partial t} d\forall + \oint_{\forall} \frac{\partial \vec{f}_c}{\partial x} d\forall + \oint_{\forall} \frac{\partial \vec{g}_c}{\partial y} d\forall = \oint_{\forall} \frac{\partial \vec{f}_v}{\partial x} d\forall + \oint_{\forall} \frac{\partial \vec{g}_v}{\partial y} d\forall + \oint_{\forall} \vec{S} d\forall \tag{4}$$

Using the divergence theorem, the volume integrals associated with the flux terms are converted to surface integrals:

$$\oint_{\forall} \frac{\partial \vec{q}}{\partial t} d\forall + \oint_{S} \left(\vec{f}_c \bullet \hat{i} + \vec{g}_c \bullet \hat{j} \right) dS = \oint_{S} \left(\vec{f}_v \bullet \hat{i} + \vec{g}_v \bullet \hat{j} \right) dS + \oint_{\forall} \vec{S} d\forall \tag{5}$$

The transient and source volume integrals are approximated by the commonly employed lumped assumption and linear distribution along the face is assumed to approximate the surface integrals. Therefore, the balance equation, Eq. (5), can now be expressed in the following form:

$$\frac{\vec{q}_P - \vec{q}_P^{\,old}}{\Delta t} + \sum_{ip} \left(\vec{f}_c A_x + \vec{g}_c A_y \right)_{ip} = \sum_{ip} \left(\vec{f}_v A_x + \vec{g}_v A_y \right)_{ip} + \vec{S}_P \forall_P \tag{6}$$

Equation (6), which includes some integration point quantities, may be called the first level discrete form of the governing equations. To carry out the next step, the finite element shape functions are employed to facilitate the profile assumption part of the discretization procedure.

3 THE SECOND LEVEL OF DISCRETIZATION: FINITE-ELEMENT INTERPOLATIONS

Equation (6) contains dependent variables and their derivatives at the integration points. These quantities should be expressed in terms of the nodal dependent variables. In the proposed method, bi-linear shape functions, $\vec{N}_{ip}$, are used to estimate the variable ϕ at an arbitrary location within the element in terms of the element nodal values. Equation (7) shows the vector form of the interpolation via the element shape functions for a typical integration point shown in Fig. 2:

$$\phi_{ip} = \vec{N}_{ip} \bullet \vec{\phi} \tag{7}$$

Where

$$\vec{N}_{ip} = \begin{Bmatrix} N_1 \\ N_2 \\ N_3 \end{Bmatrix}_{ip} = \begin{Bmatrix} s \\ t \\ 1-s-t \end{Bmatrix}_{ip} , \quad \vec{\phi} = \begin{Bmatrix} \phi_1 \\ \phi_2 \\ \phi_3 \end{Bmatrix} \tag{8}$$

The vector $\vec{\phi}$ may represent the nodal values corresponding to any physical quantity of interest such as u, v or P and (s,t) are the local coordinates within an element as shown in Fig. 2.

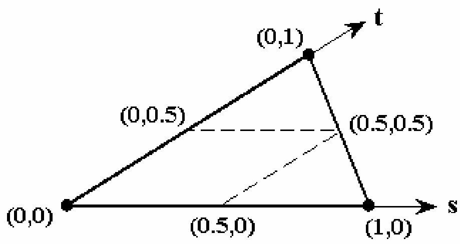

Figure 2: Local coordinates in triangular element.

The derivatives of ϕ are calculated using chain rule and Eq. (7).

$$\begin{cases} \phi_x = \dfrac{1}{J}\left(\phi_s y_t - \phi_t y_s\right) \\ \phi_y = \dfrac{1}{J}\left(\phi_t x_s - \phi_s x_t\right) \\ J = x_s y_t - x_t y_s \end{cases} \tag{9}$$

These equations can be expressed in the following compact vector form:

$$\begin{cases} \phi_x = \dfrac{1}{J}\vec{\phi}^T \underline{\underline{T}}\vec{y} \\ \phi_y = \dfrac{-1}{J}\vec{\phi}^T \underline{\underline{T}}\vec{x} \\ J = \vec{x}^T \underline{\underline{T}}\vec{y} \end{cases} \tag{10}$$

Where

$$T_{ij} = \frac{\partial N_i}{\partial s}\frac{\partial N_j}{\partial t} - \frac{\partial N_i}{\partial t}\frac{\partial N_j}{\partial s}, \quad \underline{\underline{T}} = \begin{bmatrix} 0 & 1 & -1 \\ -1 & 0 & 1 \\ 1 & -1 & 0 \end{bmatrix}, \quad \vec{x} = \begin{Bmatrix} x_1 \\ x_2 \\ x_3 \end{Bmatrix}, \quad \vec{y} = \begin{Bmatrix} y_1 \\ y_2 \\ y_3 \end{Bmatrix} \tag{11}$$

Vectors $\vec{x}^T$ and $\vec{\phi}^T$ are transposes of $\vec{x}$ and $\vec{\phi}$. Note that the use of linear shape functions in triangular elements results in a constant uniform estimation of the gradient within the element. The normal outward area vector at each integration point is calculated as follows:

$$\left(A_x\right)_{ip} = \vec{\alpha}_{ip} \bullet \vec{y}, \quad \left(A_y\right)_{ip} = -\vec{\alpha}_{ip} \bullet \vec{x} \tag{12}$$

Where

$$\vec{\alpha}_{ip} = \vec{N}\left(s_1, t_1\right) - \vec{N}\left(s_2, t_2\right) \tag{13}$$

7.2 Convection Modeling

Equation (6) contains convective fluxes which are nonlinear. Discretization of the continuity equation will be discussed later. Now we want to introduce a suitable interpolation strategy for the velocities in the convection terms in the momentum equations such that the physical propagation of the signals in the flow are simulated correctly. The proposed interpolation is dictated by the direction of the flow at the integration point and the element Peclet number. Along the local flow direction, a weighted average of the upwind and central schemes, related to the element Peclet number, is used. Also, the added numerical diffusion due to the first order upwinding in this scheme, enhances the numerical stability. For an arbitrary quantity ϕ at the integration point ip, the convection flux is calculated as follows:

$$\phi_{ip} = \phi_{up} + \gamma_{ip}\left(\vec{N}_{ip} \bullet \vec{\phi} - \phi_{up}\right), \qquad 0 \le \gamma_{ip} \le 1 \tag{14}$$

The power-low scheme can be used for the calculation of γ_{ip}

$$\gamma_{ip} = \max\left(0, \left(1 - 0.1Pe_{ip}\right)^5\right) \tag{15}$$

Where

$$Pe_{ip} = \frac{\rho_{ip}\left|\vec{U}_{ip}\right|\delta L}{\mu}, \qquad \left|\vec{U}_{ip}\right| = \sqrt{u_{ip}^2 + v_{ip}^2} \tag{16}$$

The location of ϕ_{up} is shown in Fig. 3, and δL is the average of three sides of the triangle. ϕ_{up} is calculated from linear interpolation between ϕ_a and ϕ_b which are shown in Fig. 3 as follows

$$\phi_{up} = \frac{l_a}{l_a + l_b}\phi_a + \frac{l_b}{l_a + l_b}\phi_b \tag{17}$$

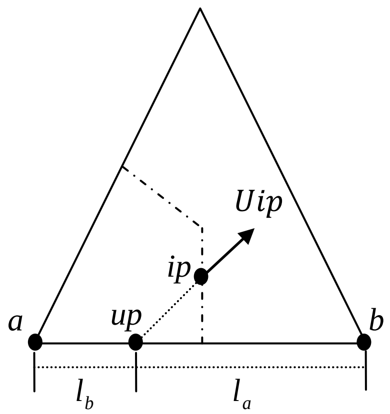

Figure 3: Location of the upwind point for an integration point.

7.2 Diffusion Modeling

The diffusion fluxes at the right hand side of Eq. (5) are the components of stress tensor which are related to the derivatives of the components of velocity vector. Using Eq. (10) which describes the derivatives in vector form at each integration point in terms of nodal values, the diffusion term τ_{xx} in Eq. (3), can be represented by the following expression:

$$\left(\tau_{xx}\right)_{ip} = \left[\frac{2\mu}{3J}\left(2\vec{u}^{T}\underline{\underline{T}}\vec{y} + \vec{v}^{T}\underline{\underline{T}}\vec{x}\right)\right]_{ip} \tag{18}$$

Other components of diffusion fluxes can be obtained in a similar manner.

4 PRESSURE-VELOCITY COUPLING METHOD

A major consideration in the numerical modeling of an incompressible flow is to avoid the checkerboard symptom. Such undesirable solutions may appear if the continuity equation is descretized with no attention to the modeling of the effect of the pressure field. In the original governing equations pressure does not appear explicitly in the continuity equation and there exists no explicit coupling between the pressure and velocity in the continuity equation. Patankar and Spalding[2] used staggered grid formulation to enforce the correct relationship between the nodal values of pressure and velocity. In this formulation pressure is stored at the center and velocities at the faces of the control volumes. However, in unstructured grid the collocated storage scheme is preferred for the sake of convenience as pointed out previously.

In the proposed method in this paper the integration point velocity components in the continuity equation are discretized using the momentum interpolation technique. Consequently, the nodal pressure appears in the control volume continuity equation. Consider the discretized momentum equation for a node P:

$$\begin{cases} u_P = \dfrac{\sum a_{nb}^{u} u_{nb}}{a_P^{u}} - \dfrac{\forall_P}{a_P^{u}}\dfrac{\partial P}{\partial x} \\ v_P = \dfrac{\sum a_{nb}^{v} v_{nb}}{a_P^{v}} - \dfrac{\forall_P}{a_P^{v}}\dfrac{\partial P}{\partial y} \end{cases} \tag{19}$$

The dimension of the first term on the right hand side of Eq. (19) is the same as the dimension of the velocity and therefore it is called the pseudo-velocity. We can rewrite Eq. (19) at an integration point in terms of the pseudo-velocities u^* and v^* as follows:

$$\begin{cases} u_{ip} = u_{ip}^{*} - d_{ip}^{u}\left.\dfrac{\partial P}{\partial x}\right|_{ip} \\ v_{ip} = v_{ip}^{*} - d_{ip}^{v}\left.\dfrac{\partial P}{\partial y}\right|_{ip} \end{cases} \tag{20}$$

The coefficients d_{ip}^{u} and d_{ip}^{v} are interpolated from the corresponding nodal values in Eq. (19). Pseudo-velocities are computed from the modified momentum equations with the pressure derivative terms removed:

$$\begin{cases} \sum_{ip} \rho\left(u^* A_x + v^* A_y\right) u_{ip}^* - \sum_{ip} \left(A_x \tau_{xx}^* + A_y \tau_{xy}^*\right)_{ip} = S_u \forall_P \\ \sum_{ip} \rho\left(u^* A_x + v^* A_y\right) v_{ip}^* - \sum_{ip} \left(A_x \tau_{yx}^* + A_y \tau_{yy}^*\right)_{ip} = S_v \forall_P \end{cases} \tag{21}$$

By substituting the momentum interpolation, Eqs. (20), into the continuity equation, the following equation constraining the element nodal pressures is obtained:

$$\sum_{ip} \vec{D}_{ip}^{mp} \bullet \vec{P} = \sum_{ip} \rho\left(A_x u^* + A_y v^*\right)_{ip} - S_m \forall_P \tag{22}$$

Where

$$\vec{D}_{ip}^{mp} = \frac{\rho}{J}\left(A_x d^u \underline{\underline{T}}\vec{y} - A_y d^v \underline{\underline{T}}\vec{x}\right)_{ip}, \quad \vec{P} = \begin{Bmatrix} P_1 \\ P_2 \\ P_3 \end{Bmatrix} \tag{23}$$

5 BOUNDARY CONDITIONS

Achieving a truly divergence free velocity field is one of the most important goals in collocated numerical solution schemes for incompressible flow problems[18]. There are three types of boundary conditions in this study which are classified as inlet, outlet and solid wall boundary conditions. Along a solid wall and an inlet, the nodal velocity is specified and there is no need to solve the momentum equations, but the pressure is unknown and a zero Neumann boundary condition for the pressure should be imposed. Implementation of this boundary condition needs more attention to the pressure equation. Remember that the continuity equation was converted into the pressure equation through the momentum interpolation for the mass velocities at integration points.

Consider the boundary node B in Fig. 4. The integration points ip_1 and ip_8 are located at the boundary on which the velocity is specified and, therefore, there is no need to use the momentum interpolation to substitute the velocity by pseudo-velocity and pressure gradient. Thus the pressure equation for the boundary nodes on a solid wall or an inlet can be expressed as follows:

$$\sum_{ip\_int} \vec{D}_{ip}^{mp} \bullet \vec{P} = \sum_{ip\_int} \rho\left(A_x u^* + A_y v^*\right)_{ip} - S_m \forall_P + \sum_{ip\_bou} \rho\left(A_x u + A_y v\right)_{ip} \tag{24}$$

Where ip_int are the internal integration points around node B for which the momentum interpolation has to be used, and ip_bou are the boundary integration points around node B with known velocity values. As a result, there is no need for any additional treatment for the pressure on the boundary because this method inherently includes the Neumann boundary condition for the pressure. When the values of velocity and pseudo-velocity in Eq. (20) are the same, the pressure gradient is zero. Therefore, implementation of the Dirichlet velocity boundary condition is equivalent to imposing the Neumann boundary condition for the pressure. This makes sense considering the tight relation between the pressure and velocity in incompressible flows.

For the outlet boundary condition extrapolation can be used or if the length of the channel in an internal flow problem is sufficiently long, the assumption of fully developed flow is a reasonable choice.

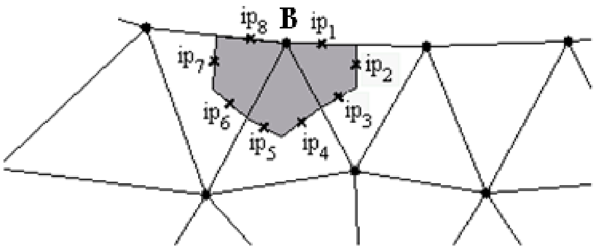

Figure 4: A typical boundary node.

6 SOLUTION ALGORITHM

The overall solution algorithm, which is iterative because of the nonlinearity of the set of equations, can be described as follows:

- Make an initial guess for the pressure and velocity fields.
- Solve Eqs. (21) to obtain the pseudo-velocities u^* and v^*.
- Solve Eq. (22) to obtain the pressure P.
- Calculate the nodal velocities from Eqs. (20) employed at nodal points.
- Go to step 2 and iterate until a convergence criterion is satisfied.

7 RESULTS

Two-dimensional lid-driven cavity flow is commonly a benchmark problem for incompressible solvers. The unit square cavity is composed of one moving upper wall and three stationary walls. The 2-D unstructured grid is generated using GAMBIT software and contains 22464 triangular cells. The flow is computed for Re = 400 and Re = 1000 and compare with Ghia et al.[19] results obtained on a 129×129 structured Grid (16641 rectangular cells). Figures 5 and 6 show cavity results for Re = 400.

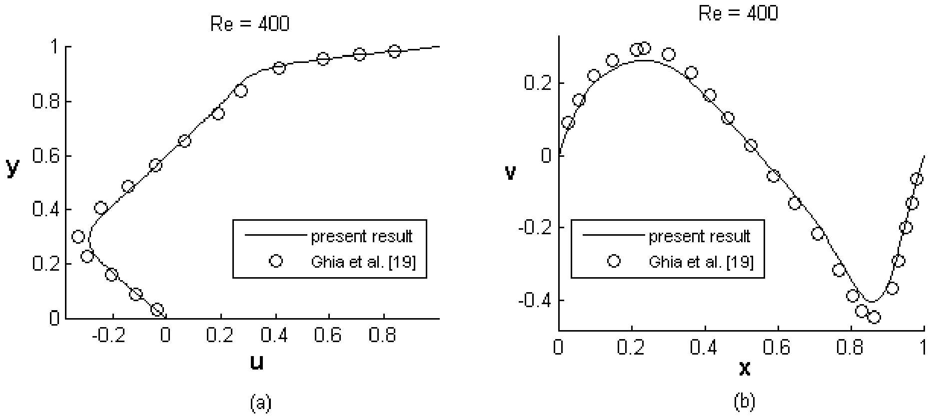

Figure 5: Cavity Re = 400, (a) u velocity along the vertical centerline; (b) v velocity along the horizontal centerline.

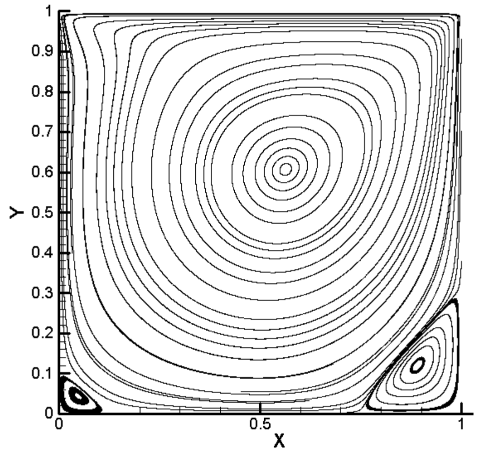

Figure 6: Streamlines for the Re = 400 case.

Figures 7 and 8 show cavity results for Re = 1000.

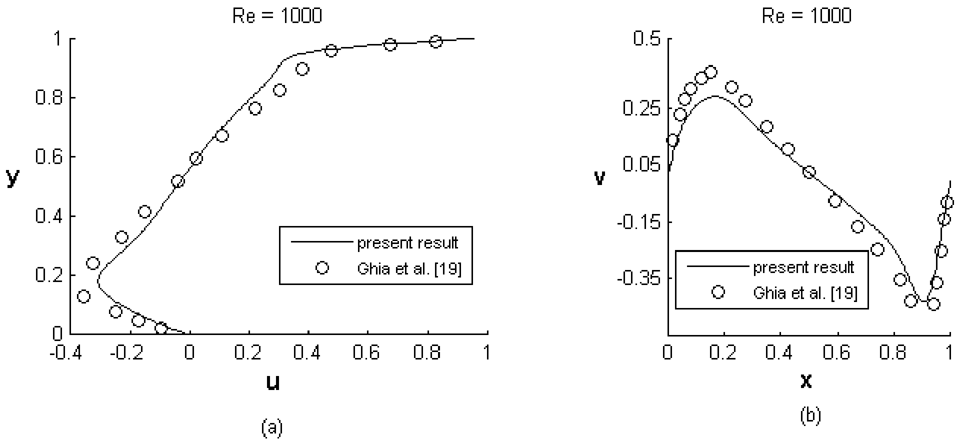

Figure 7: Cavity Re = 1000, (a) u velocity along the vertical centerline; (b) v velocity along the horizontal centerline.

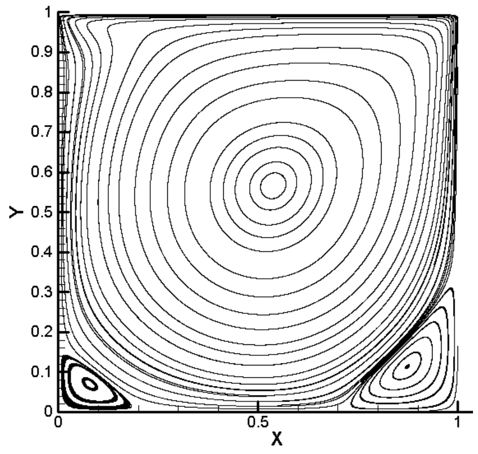

Figure 8: Streamlines for the Re = 1000 case.

Figure 9 shows the streamline for Re = 3200. Due to the first order upwinding in the proposed scheme, the solutions are not accurate for higher Reynolds, even though the qualitative behavior of streamlines is satisfactory.

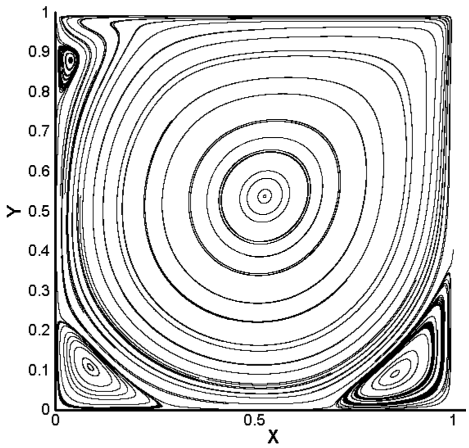

Figure 9: Streamlines for the Re = 3200 case.

8 CONCLUSION

A numerical algorithm has been proposed for solution of incompressible viscous flows. The algorithm employs a control-volume finite element method on unstructured grids. The method resolves the pressure-velocity decoupling issue by a method close to the well-known momentum interpolation scheme. Numerical results are in good agreement with those of a benchmark lid-driven cavity problem.

REFERENCES

[1] S.V. Patankar, Numerical Heat Transfer and Fluid Flow, *Hemisphere, Washington D.C.*, pp. 113-125 (1980)

[2] S.V. Patankar, D.B. Spalding, A Calculation Procedure for Heat, Mass and Momentum Transfer in Three-Dimensional Parabolic Flows, *Int. J. Heat Mass Transfer,* **15,** pp.1787-1806 (1972)

[3] C. M. Rhie and Chow, Numerical study of the Turbulent Flow past an Airfoil with Trailing Edge Separation, *AIAA J.*, **21**, pp. 1525-1532 (1983)

[4] A. J. Chorin, Numerical Solution of the Navier-Stokes Equations, *Math. Comp*., **22**, pp. 745-762 (1968)

[5] Z. Mazhar, A Procedure for the Treatment of the Velocity-Pressure Coupling Problem in Incompressible Fluid Flow, *Numerical Heat Transfer, part B*, **39**, pp. 91-100 (2001)

[6] M. Darwish, I. Sraj and F. Moukalled, A Coupled Incompressible Flow Solver on Structured Grids, *Numerical Heat Transfer, Part B,* **52,** pp. 353-371 (2007)

[7] I. Ammara and C. Masson, Development of a Fully Coupled Control-Volume Finite Element Method for the Incompressible Navier-Stokes Equations, *Int. J. Numer. Meth. Fluids,* **44,** pp. 621-644 (2004)

[8] S. R. Mathur and J. Y. Murthy, A Pressure-Based Method for Unstructured Meshes, *Numer. Heat Transfer*, **31,** pp.195-215 (1997)

[9] N. Lambropoulos, E. S. Politis, K. C. Giannakoglou and K. D. Papailiou, Co-located Pressure-Correction Formulation on Unstructured 2-D Grids, *Computational Mechanics*, **27,** pp.258-264 (2001)

[10] A. Dalal, V. Eswaran and G. Biswas, A Finite-Volume Method for Navier-Stokes Equations on Unstructured Meshes, *Numerical Heat Transfer, part B,* **54,** pp.238-259 (2008)

[11] A.W. Date, Solution of Transport Equations on Unstructured Meshes with Cell-Centered Colocated Variables. Part I: Discretization, *Int. J. Heat Mass Transfer*, **48,** pp. 1117-1127 (2005)

[12] C.D. Perez-Segarra, C. Farre, J. Cadafalch, and A. Oliva, Analysis of Different Numerical Schemes for the Resolution of Convection-Diffusion Equations Using Finite-Volume Methods on Three-Dimensional Unstructured Grids. Part I: Discretization Schemes, *Numer. Heat Transfer B,* **49,** pp. 333-350 (2006)

[13] S. Acharya, B.R. Baliga, K. Karki, J.Y. Murthy, C. Prakash and S.P. Vanka, Pressure-Based Finite-Volume Methods in Computational Fluid Dynamics, *Journal of Heat Transfer,* **129,** pp. 407-424 (2007)

[14] D. Kwak, C. Kiris and C.S. Kim, Computational Challenges of Viscous Incompressible Flows, *Computers & Fluids,* **34,** pp. 283-299 (2005)

[15] B. R. Baliga, A Control-Volume-Based Finite Element Method for Convective Heat and Mass Transfer, Ph. D. Thesis, *University of Minnesota, Minneapolis* (1978)

[16] G.E. Schneider and M.J. Raw, Control-Volume Finite Element Method for Heat Transfer and Fluid Flow Using Co-located Variables. Part I: Computational Procedure, *Numer. Heat Transfer,* **11,** pp. 363-390 (1987)

[17] S.M.H. Karimian and G.E. Schneider, Pressure Based Control-Volume Finite Element Method for Flow at All Speeds, *AIAA Journal,* **33,** pp. 1611-1618 (1995)

[18] D. Rempfer, On Boundary Conditions for Incompressible Navier-Stokes Problems, *Applied Mechanics Reviews,* **59**, pp. 107-125 (2006)

[19] U. Ghia, K.N. Ghia and C.T. Shin, High-Resolutions for Incompressible Flow Using the Navier-Stokes Equations and a Multigrid Method, *J. Comput. Phys,* **48,** pp. 387-411 (1982)